

# Quaternary Ammonium Salts Based on (-)-Borneol as Effective Inhibitors of Influenza Virus

Anastasiya Sokolova (✉ [a.s\\_sokolova@mail.ru](mailto:a.s_sokolova@mail.ru))

Vorozhtsov Novosibirsk Institute of Organic Chemistry SB RAS: Novosibirskij institut organicskoj himii imeni N N Vorozcova SO RAN <https://orcid.org/0000-0001-5227-9996>

Olga Yarovaya

Vorozhtsov Novosibirsk Institute of Organic Chemistry SB RAS: Novosibirskij institut organicskoj himii imeni N N Vorozcova SO RAN

Darya Baranova

Vorozhtsov Novosibirsk Institute of Organic Chemistry SB RAS: Novosibirskij institut organicskoj himii imeni N N Vorozcova SO RAN

Anastasiya Galochkina

Sankt-Peterburgskij naučno-issledovatel'skij institut èpidemiologii i mikrobiologii imeni Pastera: Sankt-Peterburgskij naucno-issledovatel'skij institut epidemiologii i mikrobiologii imeni Pastera

Marina Kireeva

Saint-Petersburg State University: Sankt-peterburgskij gosudarstvennyj universitet

Anna Shtro

Sankt-Peterburgskij naučno-issledovatel'skij institut èpidemiologii i mikrobiologii imeni Pastera: Sankt-Peterburgskij naucno-issledovatel'skij institut epidemiologii i mikrobiologii imeni Pastera

Sophia Borisevich

Ufa Institute of Chemistry RAS: Ufimskij Institut himii RAN

Yuriy Gatilov

Novosibirsk Institute of Organic Chemistry

Vladimir Zarubaev

Sankt-Peterburgskij naučno-issledovatel'skij institut èpidemiologii i mikrobiologii imeni Pastera: Sankt-Peterburgskij naucno-issledovatel'skij institut epidemiologii i mikrobiologii imeni Pastera

Nariman Salakhutdinov

Novosibirsk Institute of Organic Chemistry

---

## Research Article

**Keywords:** borneol, camphor, quaternary ammonium salts, influenza virus inhibitors

**Posted Date:** February 25th, 2021

DOI: <https://doi.org/10.21203/rs.3.rs-246928/v1>

**License:**  This work is licensed under a Creative Commons Attribution 4.0 International License.

[Read Full License](#)

---

# Abstract

A new compounds containing 1,7,7-trimethylbicyclo[2.2.1]heptane fragment has been found to exhibit potent inhibitory activity against the influenza A(H1N1) virus. The most potent antiviral compound **10a** is a quaternary ammonium salt based on (-)-borneol, with a therapeutic index of more than 500. Mechanism-of-action studies for compound **10a** were performed. The compound appeared the most effective when added at the early stages of viral life cycle. In direct hemagglutinin inhibition tests the agent, **10a**, was shown to decrease the activity of hemagglutinin of influenza virus A/Puerto Rico/8/34. According to the results of molecular modelling, the lead-compound, **10a**, can attach at the binding sites of the stem part of the HA. These results prove that monoterpenoids with 1,7,7-trimethylbicyclo[2.2.1]heptane fragment are prospective natural compounds for the development of antiviral agents.

## 1. Introduction

Influenza represents a serious challenge to the medical science and healthcare systems worldwide. Influenza A virus belongs to *Orthomyxoviridae* family, it is an enveloped virus containing a segmented single-stranded RNA genome of negative polarity. Because of its segmented nature and high rate of polymerase errors, influenza virus demonstrates a high rate of mutations leading to emergence of novel variants, including those with pandemic potential. Four influenza pandemics have occurred in the past 100 years: H1N1 Spanish influenza in 1918, H2N2 Asian influenza in 1957, H3N2 Hong Kong influenza in 1968, and H1N1 swine influenza in 2009 [1]. Influenza infection results in high morbidity and about 250,000 to 500,000 fatal cases annually [2]. It can lead to multiple complications for the patient, resulting in multi-organ failure, which leads to a high pathogenicity and mortality [3]. Usually, influenza A infects the upper respiratory tract and causes mild respiratory symptoms. In risk groups, however, the infection spreads to the lower respiratory tract which results in viral pneumonia. This occurs mainly in patients with a weakened immune system, including the elderly. Current treatments have limited effectiveness when administered in the late phase of the disease and this highlights the need for additional therapies [4].

Four classes of antiviral drugs are approved for the treatment of influenza: the M2 ion channel inhibitors (adamantane derivatives and isoborneol derivative, deitiforin), neuraminidase inhibitors, membrane fusion inhibitors, and RNA-dependent RNA polymerase inhibitors (Figure 1). Of these, only the adamantane derivatives (amantadine and rimantadine) and neuraminidase inhibitors (oseltamivir, zanamivir, peramivir) are approved by the Food and Drug Administration (FDA). In addition, laninamivir, a long-acting neuraminidase inhibitor was launched in Japan for the treatment of influenza A and B in 2010. Favipiravir (T-705) and ribavirin are nucleoside analogues with a broad-range of anti-viral activity. They inhibit viral polymerase enzymatic complex and induce lethal mutagenesis in the viral genome, thus decreasing the infectivity of viral progeny [5]. Umifenovir (arbidol), an inhibitor of the fusion of the viral envelope with the endosome membrane, was developed in Russia and recently approved for the

treatment of influenza in China [6]. Recently, inhibitor of viral endonuclease activity baloxavir marboxil (Xofluza®) was approved for treatment of influenza infection [7].

As mentioned above, owing to the error-prone activity of viral polymerase and segmented genome, the influenza virus is able to select drug-resistant variants. In particular, due to the widespread resistance of influenza viruses to adamantane derivatives, the M2 ion channel inhibitors are not currently recommended for therapy [8]. The fast spreading resistance to oseltamivir (Tamiflu) has also been observed [9]. Since the influenza virus is capable of developing resistance to the available antivirals, there is, therefore, a real need for the development of novel inhibitors for the influenza virus.

In previous studies, our research group showed that (+)-camphor and (-)-borneol are hopeful scaffolds for the synthesis of antiviral drugs. In particular, the camphor imine derivatives including compounds 1-2 were found to possess high antiviral activity (Figure 2) [10,11,12]. The hit compound Camphecene (Camphecin®) was shown to directly inhibit the acid-induced membrane-disrupting activity of the viral haemagglutinin of the influenza A viruses [13]. Also, it was shown that dimeric quaternary ammonium camphor derivatives exhibit high efficiency as an agent inhibiting the reproduction of the influenza virus (strain A/Puerto Rico/8/34 (H1N1)) the most active among them is compound 3 [14]. Moreover from the last decade, our group has been involved in the synthesis of biologically significant novel (-)-borneol derivatives. We discovered several borneol ester molecules with activity against Ebola virus (EBOV) and Marburg virus (MARV) and influenza virus, for example, compounds 4-5 [15,16,17]. Moreover, we have shown that the possible mechanism of inhibition of EBOV is binding to the active site of EBOV glycoprotein [18]. The filovirus family, which includes EBOV and MARV, and the orthomyxovirus family, which includes the influenza virus, belong to class I fusion proteins and have similar pre- and post-fusion forms [19]. It can be assumed that bicyclic monoterpenoids including (+)-1,7,7-trimethylbicyclo[2.2.1]heptane structural fragment is a promising scaffold for the synthesis of inhibitors of viral infections with class I fusion proteins such as influenza virus.

In the present work, we describe synthesis and results of the study of the antiviral activity of quaternary ammonium salts with groups which according to our previous research responsible for antiviral activity such as 1,7,7-trimethylbicyclo[2.2.1]heptane fragment, quaternary nitrogen atom, imino and ester group. In addition, we conducted mechanism-of-action studies for the most potent compound.

## 2. Results And Discussion

### 2.1 Chemistry

The synthesis strategy for camphor derivatives **6** and **7** was performed as outlined in Scheme 1. The key intermediate N,N-disubstituted camphor imines **1** and **2** were synthesized according to our recently reported approach [10]. Subsequently, the methylation of the tertiary amino group of the intermediates **1** and **2** was performed using excess methyl iodide, leading to the desired compounds **6** and **7** in moderate yields.

Target borneol derivatives were synthesized via a sequence of reactions starting with a commercially available (-)-borneol. Borneol derivatives 8a-c and 9a-c with tertiary amino group were prepared in two steps as previously described [18]. Subsequent methylation, using iodomethane under reflux, gave corresponding quaternary ammonium salts 10a, 10c and 11a-b (Scheme 2).

The structures of the synthesized compounds were confirmed by NMR spectra ( $^1\text{H}$ ,  $^{13}\text{C}$  NMR). The structure of compound 10a was confirmed by X-ray diffraction. The bond lengths of 10a are close to the lengths of the analogous bonds in the betaine hydrobromide and in the (cyclopentadienyl)-tricarbonyl-(2-((*-*)-borneolato)-2-oxoethyl)-molybdenum. In the crystal structure, the iodine anion is located close to the trimethylammonium group. The shortest I—H contact of 3.04 Å is shown in Figure 3. Between the cations there is a weak hydrogen bond C10-H—O=C (H—O distance 2.59 Å and C-H—O angle 167°).

## 2.2 Biological activity

### 2.2.1 Anti-influenza activity of synthesized derivatives *in vitro*

The obtained compounds have been studied as potential antiviral agents against the influenza virus A/Puerto Rico/8/34 (H1N1) (Table 1). An important characteristic of the biological activity of the studied compounds is the selectivity index (SI). The selectivity index is the ratio between the concentration of a substance that causes damage to 50% of cells ( $\text{CC}_{50}$ ) and the concentration required to reduce the viral activity by 50% ( $\text{IC}_{50}$ ). This ratio reflects the selectivity and safety of the compounds. According to the data in Table 1, transformation camphor imine derivatives 1 and 2 to corresponding quaternary ammonium salts 6 and 7 led to a loss in antiviral activity, while maintaining low toxicity. Among the (-)-borneol esters 8a-c and 9a-c with a tertiary amino group, compounds 8a,c and 9a,b showed moderate antiviral activity with a SI value higher than 2. These derivatives have been further converted to the quaternary ammonium salts 10a,c and 11a,b. In the study of the antiviral activity and toxicity of these agents, it was revealed that compound 10a showed more potent effects against influenza virus A/Puerto Rico/8/34 (H1N1).

Table 1.

Antiviral activity of the target compounds against influenza virus A/Puerto Rico/8/34 (H1N1) in MDCK cells

Compound	CC <sub>50</sub> <sup>a</sup> (μM)	IC <sub>50</sub> <sup>b</sup> (μM)	SI <sup>c</sup>
1*	>2252	52.7±0.4	43
2*	>2118	21.2±0.1	100
6	>2101	115±10	18
7	>1992	144±12	14
<b>8a</b>	597±42	163±21	4
8b	>1184	NA	-
8c	>1122	97±10	12
9a	79±6	>41	2
9b	814±65	36±5	23
9c	34±2	>14	3
10a	1311±126	2.4±0.4	546
<b>10c</b>	264±15	>117	2
<b>11a</b>	850±38	316±40	3
<b>11b</b>	69±6	>37	2
Rimantadine	335±27	67.0±4.9	5
Amantadine	284±21	64.2±4.7	4
Deitiforine	1266±81	209±15	6
Ribavirin	>2000	24.6	>81

<sup>a</sup> CC<sub>50</sub> is cytotoxic concentration; the concentration resulting in the death of 50% of the cells; <sup>b</sup> IC<sub>50</sub> is 50% virus-inhibiting concentration, the concentration leading to 50% inhibition of virus replication; <sup>c</sup> SI is the selectivity index, the ratio of CC<sub>50</sub>/ IC<sub>50</sub>; \* data published previously<sup>10</sup>. NA – not active. The data presented are the mean of three independent experiments. The values for CC<sub>50</sub> and IC<sub>50</sub> are presented as the mean±error of the experiment.

Based on the *in vitro* screening we identified compound **10a** as a lead-compound since this agent demonstrated the highest SI value, and for this compound we performed the specific assays to study mechanism of action.

## 2.2.2 Time-of-addition experiments

To determine the target for the virus-inhibiting activity of compound **10a** in the virus life cycle, time-of-addition experiments were performed. The results are summarised in Figure 4. As can be suggested from the data obtained, the compound appeared to be the most effective when added at the period of 0–2 hours post infection. Over time, the efficacy of the drug decreased, and starting at 4 hours after infection, the infectious activity of the virus was not statistically different from the control values. On the basis of the results obtained, it can be assumed that the derivative of **10a** acts on the initial stage of the life cycle of the influenza virus, which involves the adsorption of virions on the surface of the target cell and penetration of the virion inside the host cell. At this stage, two viral proteins are essential. First, viral haemagglutinin provides the attachment of virions to the cell surface and fusion of the viral envelope with the endosomal membrane. Second, the virus-specific proton channel M2 conducts protons into the virion interior, thus providing acidification of the core and allowing the dissociation of ribonucleoproteins (RNPs) from the envelope structures.

## 2.2.3 Study of HA-mediated fusion process

To investigate the role of compound **10a** in HA-mediated fusion, we performed hemagglutination and hemolysis assays. In order to assess the ability of compound **10a** to interfere directly with receptor-binding site of viral hemagglutinin, we performed hemagglutination inhibition tests. Briefly, two-fold dilutions of influenza A/Puerto Rico/8/34 virus were mixed in round-bottom wells with leading compound **10a** at a range of concentrations, and chicken red blood cells (cRBCs) were then added. Wells without compound **10a** served as the control. The hemagglutinating titer of the virus was found to be 64 hemagglutinating units (HAU) per 0.2 mL. The addition of compound **10a** did not change this value even at the highest concentration used (1200 µM). Therefore, the results suggest that, compound **10a** does not inhibit the cell receptor-binding activity of viral hemagglutinin.

To determine the impact of compound **10a** on fusion activity of viral HA, the hemolysis assay was performed by using influenza A/Puerto Rico/8/34 (H1N1) virus (Figure 5). As can be seen, compound **10a** strongly decreased the ability of viral hemagglutinin to cause membrane damage, and can be considered, therefore, an effective anti-influenza membrane fusion inhibitor.

## 2.3 Molecular docking study

To characterize the details of interaction of compound **10a** directly with the hemagglutinin, the docking of the lead-compound, **10a**, into the binding site of HA was performed and the calculated docking scores were compared with the values for the well-known HA inhibitor tert-butylhydroquinone, TBHQ, and the new anti-influenza drug camphecene (Figure 6). Two binding sites of HA were considered; the first was located in the binding region for TBHQ [20] and the second was found near a site of proteolysis, where camphecene binds [21].

The lead-compound, **10a**, can bind to both sites in HA. Firstly, compound **10a** can fit in the space between the two monomers (TBQH-site) and form hydrogen and salt bridges with LYS58 and ASP27, respectively. Secondly, compound **10a** can bind at the site of proteolysis of HA, in the so-called camphecene binding site (CPH-site) (Figure 6).

In both cases, the affinity of ligand **10a** to both binding sites is approximately equal: the docking score and LE are -6.652 and 0.370 for the TBQH-site, and -6.612 and 0.368 for the CPH-site, respectively (Figure 6). However, while in the TBQH-binding site the docking values of compound **10a** and HA inhibitors are comparable, at the CPH-site the ligand **10a** is characterised by a lower affinity compared to camphecene. In any case, derivative **10a** can bind to HA at both binding sites.

### 3. Conclusion

As a result, we have synthesized quaternary ammonium salts based on (+)-camphor and (-)-borneol. It was found that conversion of tertiary amines based on (+)-camphor to quaternary ammonium salts led to decrease antiviral activity while transformation of (-)-borneol derivatives to the corresponding salts increases inhibitory activity. Derivative **10a** showed the greatest antiviral activity with an IC<sub>50</sub> value of 2.4 µM and low toxicity with a CC<sub>50</sub> value of 1311 µM. Based on the data obtained in the mechanism-of-action studies, we propose that the virus-inhibiting activity of these compounds, in particular compound **10a**, is explained by inhibition of viral haemagglutinin. According to the results of molecular modelling, the compound binds in the stem part of hemagglutinin (HA2), which leads to blocking the process of fusion of the viral and cell membranes.

## 4. Experimental

### 4.1 Chemistry

#### 4.1.1 General

Reagents and solvents were purchased from commercial suppliers and used as received. Dry solvents were obtained according to standard procedures. Column chromatography was performed on Macherey-Nagel 60–200 µm silica gel. All the target compounds reported in this publication were of at least 98% purity. The synthesis of derivatives 1, 2 [10] and 8a-c, 9a-c [18] we described previously. Compounds 6-7, 10a,c and 11a,b have not been described previously in the literature. <sup>1</sup>H and <sup>13</sup>C NMR spectra were recorded on Bruker AV-300 (300.13 and 75.47 MHz, respectively), AV400 (400.13 and 100.78 MHz, respectively) and DRX 500 (500.13 and 125.76 MHz, respectively) spectrometers in CDCl<sub>3</sub>; chemical shifts δ, in ppm relative to residual [δ(CHCl<sub>3</sub>) 7.24, δ(CDCl<sub>3</sub>) 76.90 ppm]. The atom numbering in the compounds is given for assigning the signals in the NMR spectra and does not match the standard nomenclature of compounds. Elemental analysis was carried out using a Euro EA 3000 C, H, N, S-analyser. Analysis of Br was carried out by the mercurimetric titration method. Analysis of I was carried out by the iodometric titration method. X-ray data were collected at room temperature using a Bruker

Kappa Apex II CCD diffractometer with graphite monochromated MoKa radiation ( $\lambda = 0.71073 \text{ \AA}$ ) with  $\varphi$ ,  $\omega$ -scan method. The data were corrected for absorption using a multi-scan method with the SAINT program. The structure was solved by direct methods using SHELXS97, and refinement was carried out by a full-matrix least-squares technique, using SHELXL97. Anisotropic displacement parameters were included for all non-hydrogen atoms. All H atoms were positioned geometrically and treated as riding on their parent C atoms.

#### 4.1.2 General procedure for the target camphor derivatives 6 and 7.

A solution of compounds 1 or 2 (4 mmol) and anhydrous  $\text{CH}_3\text{CN}$  (10 mL) was treated with an excess of iodomethane and heated in a bath at 70–75°C for 6 h. The solvent was removed at reduced pressure. The resulting precipitate was purified via silica gel column chromatography ( $\text{CHCl}_3/\text{MeOH}$  eluent, (100:0→0:100)).

*N,N,N*-Trimethyl-2-((E)-((1*R,4R*)-1,7,7-trimethylbicyclo[2.2.1]heptan-2-ylidene)amino)ethanaminium iodide (6).

Yield: 46%; mp: 195–197°C;  $^1\text{H}$  NMR (400 MHz,  $\text{CDCl}_3$ , J Hz)  $\delta$  ppm: 0.67 (3H, s, Me-9), 0.84 (3H, s, Me-8), 0.88 (3H, s, Me-10), 1.17-1.27 (2H, m, H-4endo, H-5endo), 1.59-1.68 (1H, m, H-5exo), 1.77-1.86 (2H, m, H-2endo, H-4exo), 1.94-1.99 (1H, m, H-3), 2.36-2.46 (1H, m, H-2exo), 3.52 (9H, s, Me-13, Me-14, Me-15), 3.64-3.75 (2H, m, H-12), 3.85-3.95 (2H, m, H-11).  $^{13}\text{C}$  NMR (75 MHz,  $\text{CDCl}_3$ )  $\delta$ : 186.36 s (C-1), 66.41 t (C-12), 54.61 q (Me-13, Me-14, Me-15), 53.90 s (C-6), 46.97 s (C-7), 46.47 t (C-11), 43.35 d (C-3), 35.61 t (C-2), 31.54 t (C-5), 26.71 t (C-4), 19.20 q (Me-9), 18.39 q (Me-10), 10.81 q (Me-8). Anal. Calcd for  $\text{C}_{15}\text{H}_{29}\text{IN}_2$  C, 49.45; H, 8.02; I, 34.83; N, 7.69 %. Found, %: C 48.54; H 8.10; N 7.64; I 34.57.

*N,N,N*-Trimethyl-3-((E)-((1*R,4R*)-1,7,7-trimethylbicyclo[2.2.1]heptan-2-ylidene)amino)propan-1-aminium iodide (7)

Yield, 76%; mp: 231°C;  $^1\text{H}$  NMR (400 MHz,  $\text{CDCl}_3$ )  $\delta$ : 0.71 (3H, s, Me-9), 0.88 (3H, s, Me-8), 1.00 (3H, s, Me-10), 1.23-1.39 (2H, m, H-4endo, H-5endo), 1.64-1.73 (1H, m, H-5exo), 1.76-1.85 (1H, m, H-4exo), 1.98-2.02 (1H, m, H-3), 2.11 (1H, d,  $^2\text{J}=19.6$ , H-2endo), 2.20-2.29 (2H, m, H-12), 2.54-2.62 (1H, m, H-2exo), 3.41 (9H, s, Me-14, Me-15, Me-16), 3.41-3.47 (2H, m, H-13), 3.71-3.77 (2H, m, H-11).  $^{13}\text{C}$  NMR (75 MHz,  $\text{CDCl}_3$ )  $\delta$ : 191.13 s (C-1), 64.86 t (C-13), 55.35 t (C-11), 53.93 q (Me-14, Me-15, Me-16), 48.13 s (C-6), 46.96 s (C-7), 43.46 d (C-3), 36.75 t (C-2), 31.86 t (C-5), 26.56 t (C-4), 23.94 t (C-12), 19.58 q (Me-9), 18.52 q (Me-10), 11.40 q (Me-8). Anal. Calcd for  $\text{C}_{16}\text{H}_{31}\text{IN}_2$  C, 50.79; H, 8.26; I, 33.54; N, 7.40%. Found, %: C 49.68; H 8.19; N 7.32; I 33.82.

#### 4.1.3 Synthesis of(-)-borneol derivatives 10a, 10c and 11a-b.

*N,N,N*-Trimethyl-2-oxo-2-((1*S,2R,4S*)-1,7,7-trimethylbicyclo[2.2.1]heptan-2-yloxy)ethanaminium iodide (10a)

A solution of **8a** (4 mmol) and anhydrous CH<sub>3</sub>CN (10 mL) was treated with an excess of iodomethane and heated in a bath at 70–75°C for 6 h. The solvent was removed at reduced pressure. The crude product was purified by recrystallisation from CH<sub>3</sub>CN. Yield: 62%; mp: 242°C; <sup>1</sup>H NMR (400 MHz, DMSO-d6, J Hz) δ ppm: 0.83 (3H, s, Me-9), 0.87 (3H, s, Me-8), 0.89 (3H, s, Me-10), 1.04 (1H, dd, <sup>2</sup>J = 13.7, J<sub>2endo,1exo</sub>=3.5, H-2endo), 1.17-1.25 (1H, m, H-4endo), 1.27-1.37 (1H, m, H-5exo), 1.67-1.77 (2H, m, H-3, H-4exo), 1.79-1.87 (1H, m, H-5endo), 2.27-2.37 (1H, m, H-2exo), 3.24 (9H, s, Me-13, Me-14, Me-15), 4.50 (1H, AB-d, J<sub>1,2</sub>=16.7 Hz, H-12), 4.55 (1H, AB-d, J<sub>2,1</sub>=16.7 Hz, H-12), 4.95 (1H, m, H-1exo). <sup>13</sup>C NMR (125 MHz, DMSO-d6) δ: 165.28 s (C-11), 81.75 d (C-1), 62.89 t (C-12), 53.46 q (Me-13, Me-14, Me-15), 48.86 s (C-6), 47.79 s (C-7), 44.32 d (C-3), 36.03 t (C-2), 27.69 t (C-4), 26.85 t (C-5), 19.69 q (Me-9), 18.77 q (Me-10), 13.61 q (Me-8). Anal. Calcd for C<sub>15</sub>H<sub>28</sub>INO<sub>2</sub> C, 47.25; H, 7.40; I, 33.28; N, 3.67 %. Found, %: C 47.19; H 7.26; I 33.21; N 3.73.

### Crystal data for **10a**

C<sub>15</sub>H<sub>28</sub>INO<sub>2</sub>, M = 381.28, monoclinic, space group P21, a = 12.2791(5), b = 7.1686(3), c = 20.9901(9) Å, β = 101.030(2)°, V = 1813.50(13) Å<sup>3</sup>, Z = 4, D<sub>calc</sub> = 1.396 mg·m<sup>-3</sup>, μ = 1.766 mm<sup>-1</sup>. Data collection yielded 45735 reflections with θ < 30.2° resulting in 10595 unique, averaged reflections, 7365 with I > 2σ(I). Full-matrix least-squares refinement led to a final R = 0.0440, wR2 = 0.1375, GOF = 0.936 for I > 2σ(I). CCDC 1813408 contains supplementary crystallographic data for the structure. These data can be obtained free of charge via [www.ccdc.cam.ac.uk/conts/retrieving.html](http://www.ccdc.cam.ac.uk/conts/retrieving.html).

### N,N,N-Trimethyl-4-oxo-4-((1*S*,2*R*,4*S*)-1,7,7-trimethylbicyclo[2.2.1]heptan-2-yloxy)butan-1-aminium iodide (**10c**)

The synthesis of compound **10c** was performed in analogy to the synthesis compound **10a**. Yield: 43%; mp: 171.5°C; <sup>1</sup>H NMR (400 MHz, CDCl<sub>3</sub>, J Hz) δ ppm: 0.76 (3H, s, Me-9), 0.81 (3H, s, Me-8), 0.83 (3H, s, Me-10), 0.90 (1H, dd, <sup>2</sup>J=13.7, J<sub>2endo,1exo</sub>=3.5, H-2endo), 1.12-1.28 (2H, m, H-4endo, H-5exo), 1.60-1.73 (2H, m, H-3, H-4exo), 1.76-1.86 (1H, m, H-5endo), 2.00-2.10 (2H, m, H-13), 2.22-2.32 (1H, m, H-2exo), 2.49 (2H, t, J=6.7 Hz, H-12), 3.42 (9H, s, Me-15, Me-16, Me-17), 3.66-3.75 (2H, m, H-14), 4.76-4.84 (1H, m, H-1exo). <sup>13</sup>C NMR (75 MHz, CDCl<sub>3</sub>, J Hz) δ ppm: 171.9 s (C-11), 80.4 d (C-1), 65.4 t (C-14), 53.4 q (Me-15, Me-16, Me-17), 48.3 s (C-6), 47.3 s (C-7), 44.3 d (C-3), 36.2 t (C-2), 29.4 t (C-12), 27.4 t (C-4), 26.5 t (C-5), 19.2 q (Me-9), 18.3 q (Me-10), 18.0 t (C-13), 13.1 q (Me-8). Anal. Calcd for C<sub>17</sub>H<sub>32</sub>INO<sub>2</sub> C, 49.88; H, 7.88; N, 3.42 %. Found, %: C 49.87; H 7.71; N 3.20.

### N,N-Diethyl-N-methyl-2-oxo-2-((1*S*,2*S*,4*S*)-1,7,7-trimethylbicyclo[2.2.1]heptan-2-yloxy)ethanaminium iodide (**11a**)

A solution of **9a** (0.2 mmol) and anhydrous CH<sub>3</sub>CN (5 mL) was treated with an excess of iodomethane and refluxed for 6 h. The solvent was removed at reduced pressure. The crude product was purified by recrystallisation from CH<sub>3</sub>CN. Yield: 51%; mp: 159.2-159.3°C; <sup>1</sup>H NMR (400 MHz, CDCl<sub>3</sub>, J Hz) δ ppm: 0.80

(3H, s, Me-9), 0.83 (3H, s, Me-8), 0.85 (3H, s, Me-10), 1.01 (1H, dd,  $^2J=13.7$ ,  $J_{2\text{endo},1\text{exo}}=3.5$ , H-2endo), 1.17-1.35 (2H, m, H-4endo, H-5exo), 1.42 (6H, t,  $J=7.2$ , Me-15, Me-16), 1.62-1.76 (2H, m, H-3, H-4exo), 1.78-1.90 (1H, m, H-5endo), 2.25-2.38 (1H, m, H-2exo), 3.48 (3H, s, Me-17), 3.75-3.95 (4H, m, H-13, H-14), 4.55 (2H, AB, H-12), 4.91-5.00 (1H, m, H-1exo).  $^{13}\text{C}$  NMR (100 MHz,  $\text{CDCl}_3$ , J Hz)  $\delta$  ppm: 164.3 s (C-11), 83.2 d (C-1), 58.7 t (C-12), 57.8 t (C-13, C-14), 48.8 s (C-6), 48.6 q (Me-17), 47.8 s (C-7), 44.4 d (C-3), 36.2 t (C-2), 27.6 t (C-4), 26.8 t (C-5), 19.4 q (Me-9), 18.5 q (Me-10), 13.5 q (Me-8), 8.3 q (Me-15, Me-16). Anal. Calcd for  $\text{C}_{17}\text{H}_{32}\text{INO}_2$  C 49.87; H 7.71; N 3.20 %. Found, %: C 50.29; H 8.08; N 3.14.

**N,N-Diethyl-N-methyl-3-oxo-3-((1S,2S,4S)-1,7,7-trimethylbicyclo[2.2.1]heptan-2-yloxy)propan-1-aminium iodide (11b)**

The synthesis of compound **11b** was performed in analogy to the synthesis compound **11a**. Yield: 53%; mp: 147.3-147.7°C;  $^1\text{H}$  NMR (400 MHz,  $\text{CDCl}_3$ , J Hz)  $\delta$  ppm: 0.81 (3H, s, Me-9), 0.84 (3H, s, Me-8), 0.86 (3H, s, Me-10), 1.00 (1H, dd,  $^2J=13.7$ ,  $J_{2\text{endo},1\text{exo}}=3.5$ , H-2endo), 1.21-1.34 (2H, m, H-4endo, H-5exo), 1.42 (6H, t,  $J=7.2$ , Me-16, Me-17), 1.65-1.76 (2H, m, H-3, H-4exo), 1.82-1.91 (1H, m, H-5endo), 2.26-2.36 (1H, m, H-2exo), 2.96 (2H, t,  $J=7.1$  Hz, H-12), 3.29 (3H, s, Me-18), 3.59-3.71 (2H, m, H-14, H-15), 3.75 (2H, t,  $J=7.1$ , H-13), 4.85-4.90 (1H, m, H-1exo).  $^{13}\text{C}$  NMR (100 MHz,  $\text{CDCl}_3$ , J Hz)  $\delta$  ppm: 169.5 s (C-11), 81.9 d (C-1), 57.3 t (C-14, C-15), 56.0 t (C-13), 48.6 s (C-6), 48.2 q (Me-18), 47.8 s (C-7), 44.5 d (C-3), 36.4 t (C-2), 28.1 t (C-12), 27.7 t (C-4), 26.9 t (C-5), 19.5 q (Me-9), 18.6 q (Me-10), 13.5 q (Me-8), 8.3 q (Me-16, Me-17). Anal. Calcd for  $\text{C}_{18}\text{H}_{34}\text{INO}_2$  C 51.06; H 8.09; N 3.42 %. Found, %: C 50.50; H 8.22; N 3.17.

## 4.2 Biological assays

### 4.2.1 Cells and viruses

Influenza virus A/Puerto Rico/8/34 (H1N1) was obtained from the collection of viruses of St Petersburg Pasteur Institute, Russia, and used in the study. Prior to the experiment, the virus was propagated in the allantoic cavity of 10-12 days-old chicken embryos for 48 hr at 36°C. Infectious titer of the virus was determined in MDCK cells (ATCC # CCL-34) in 96-wells plates in alpha-MEM medium (Biolot, St.-Petersburg, Russia).

### 4.2.2 Cytotoxicity assay

The microtetrazolium test (MTT) was used to study the cytotoxicity of the compounds. Briefly, a series of threefold dilutions of each compound in MEM were prepared. The MDCK cells were incubated for 48 h at 36°C in 5%  $\text{CO}_2$  in the presence of the dissolved substances. The cells were washed twice with phosphate-buffered saline (PBS), and a solution of 3-(4,5-dimethylthiazolyl-2)-2,5-diphenyltetrazolium bromide (ICN Biochemicals Inc. Aurora, Ohio) (0.5  $\mu\text{g}/\text{mL}$ ) in PBS was added to the wells. After 1 h incubation, the wells were washed, and the formazan residue was dissolved in DMSO (0.1 mL per well). The optical density in the wells was then measured on a Victor2 1440 multifunctional reader (Perkin Elmer, Finland) at a wavelength of 535 nm and plotted against the concentration of compounds. Each

concentration was tested triplicate. The 50% cytotoxic concentration ( $CC_{50}$ ) of each compound was calculated from the data obtained.

#### **4.2.3 *In vitro* antiviral activity**

The compounds were dissolved in 0.1 mL DMSO to prepare stock solutions, and final solutions (1000.0–4.0  $\mu$ M) were prepared by adding MEM with 1  $\mu$ g/mL trypsin. The compounds were incubated with MDCK cells for 1 h at 36°C. Each concentration of the compounds was tested in triplicate. The cell culture was then infected with the influenza virus A/Puerto Rico/8/34 (H1N1) (MOI 0.01) for 24 h at 36°C in the presence of 5% CO<sub>2</sub>. A virus titre in the supernatant was determined by a haemagglutination test after cultivation of the virus in the MDCK cells for 48 h at 36°C in the presence of 5% CO<sub>2</sub>. Rimantadine, amantadine, deitiforin, and ribavirin were used as reference drugs. For calculations, the virus titre was expressed as per cent of the titre in control wells without compounds. The 50% inhibiting concentrations (IC<sub>50</sub>) and the selectivity index (SI, the ratio of CTC<sub>50</sub> to IC<sub>50</sub>) were calculated from the obtained data.

#### **4.2.4 Time-of-addition experiments**

To determine which stage of the viral life cycle is affected by the compound, cells were seeded into 24-wells plates and incubated with the influenza virus A/Puerto Rico/8/34 (H1N1) (m.o.i. 10) for 1 h at 4°C. After washing the non-absorbed virions for 5 min with MEM, the plates were incubated for 8 h at 36°C at 5% CO<sub>2</sub>. The starting point of this incubation was referred to as 0 hours. The cells were treated with compound 11 for the following time periods: -2 to -1 (before infecting); -1 to 0 (simultaneously to absorption); 0 to 2; 2 to 4; 4 to 6; 6 to 8; and -2 to 8 hours. In each case after incubation the compound was removed, and cells were washed for 5 min with MEM. After 8 hours of growth, the infectious titer of the virus was determined in the culture medium, as described above.

#### **4.2.5 Hemagglutination inhibition assay and haemolysis assay**

In order to assess the ability of compounds to interfere directly with HA receptor binding, we performed hemagglutination inhibition test. Two-fold dilutions of influenza A/Puerto Rico/8/34 virus-containing culture medium (1:8 to 1:256) were mixed with leading compound at a range of concentrations and incubated for 1 hour at 36°C at 5% CO<sub>2</sub> followed by adding equal volume of 1% chicken erythrocytes. After incubation for 1 hour at 20°C the results were checked visually. Anti-hemagglutinin activity was evaluated by the ability of specimens to prevent virus-driven hemagglutination.

The membrane-disrupting activity of viral hemagglutinin was measured according to Maeda and Ohnishi [22] with slight modifications. Briefly, chicken erythrocytes were washed twice with PBS and resuspended to make a 0.75% (vol./vol.) suspension in PBS, which was stored at 4°C until use. One hundred microliters of compound diluted in PBS to appropriate concentrations was mixed with an equal volume of the influenza virus (128 hemagglutinating units per 0.1 mL), or PBS for negative control. After incubating the virus-compound mixture at room temperature for 30 min, the mixture was mixed with 300  $\mu$ L of 0.75% chicken erythrocytes. Mixture was incubated for 1 hour at +4°C for absorption of virions on erythrocytes.

500 µL of MES buffer (0.1M MES, 0.15M NaCl, 0.9mM CaCl<sub>2</sub>, 0.5mM MgCl<sub>2</sub>, pH 5.0) was added, mixed and incubated for 1 hour at 37°C for HA acidification and hemolysis. To separate non-lysed erythrocytes, tubes were centrifuged at the end of incubation at 1,200 rpm for 6 min. After sedimentation of erythrocytes 100 µL of supernatant were transferred into the wells of a flat-bottom plate and optical density in the wells was measured at 405 nm. The activity of compounds was considered as their ability to suppress the destruction of membranes and thus decrease the concentration of free hemoglobin and optical density in the wells comparing to the control wells without additives. The activity of HA was calculated as  $(OD_c - ODb) / (OD_p - ODb) \times 100\%$ , where OD<sub>p</sub> and OD<sub>s</sub> are mean optical densities in the wells with PBS and compound under investigation, correspondingly, and ODb (background) is mean optical density in the wells with erythrocytes, but without virus and compounds. The activity of HA in control wells without any virus was calculated by comparison to HA activity of influenza A virus.

#### 4.3 Molecular docking study

The crystal structure of haemagglutinin was used for the docking procedure (PDB code: 3LZG) [23]. The geometric parameters of HA protein were optimised using the OPLS3 force field algorithm [24].

To find the active site in the HA corresponding to 3LZG PDB code, we analysed the binding site of the native ligand well-known in the HA inhibitor, TBHQ in 3EYM<sup>20</sup> PDB code. This necessary procedure is one of the stages of molecular modelling. The TBHQ binding site is located at the interface between two monomers of the HA trimer. Based on an analysis of the active site, the area around the native ligand, with a radius of 5 Å was selected. The functional amino acid sequence was compared in two PDB codes and the area of the TBHQ binding was detected in the protein 3LZG and was used for further docking procedures

The CPH-binding site was arranged at the site of proteolysis next to the amino acid valine at position 615 (the numbering corresponds to the 1RU7 [25] code). Details have been previously described [21].

Ligand preparation (optimisation, which took into account all possible conformations of the ligand) and all the docking procedures were carried out using the Schrodinger Small-Molecule Drug Discovery Suite 2018-4, Schrödinger, LLC, New York, NY, 2018 program packages. The docking was performed under the following conditions: ligand and protein are flexible and induced fit docking protocols were used for standard prediction accuracy.

## Declarations

### Conflicts of interest

The authors declare no competing interests.

### Ethical approval

This article does not contain any studies with human participants or animals performed by any of the authors.

## Acknowledgements

The authors would like to acknowledge the Multi-Access Chemical Service Centre SB RAS for spectral and analytical measurements. This work has been supported by a Russian Scientific Foundation grant 19-73-00125. All the calculations were carried out on a cluster in the regional centre for shared computer equipment at the Ufa Institute of Chemistry UFRC RAS.

## References

1. Paules C., Subbarao K. (2017) Influenza. *The Lancet* 390: 697–708. DOI: 10.1016/S0140-6736(17)30129-0
2. Fiore A. E., Shay D. K., Broder K., Iskander J. K., Uyeki T. M., Mootrey G., Bresee J. S., Cox N. J. (2008) Prevention and Control of Seasonal Influenza with Vaccines. *MMWR Recomm. Rep.* 57:1–60.
3. Yuan S. (2013) Drugs to cure avian influenza infection multiple ways to prevent cell death. *Cell Death Dis.* 4: 835. DOI: 10.1038/cddis.2013.367
4. Armstrong S. M., Darwish I., Lee W. L. (2013) Drugs to cure avian influenza infection multiple ways to prevent cell death. *Virulence* 4: 537–542. DOI: 10.1038/cddis.2013.367
5. Baranovich T., Wong S. S., Armstrong J., Marjuki H., Webby R. J., Webster R. G., Govorkova E. A. (2013) Favipiravir Induces Lethal Mutagenesis in Influenza A H1N1 Viruses In Vitro. *J. Virol.* 87: 3741–3751. DOI: 10.1128/jvi.02346-12
6. Sun Y., He X., Qiu F., Zhu X., Zhao M., Li-Ling J., Su X., Zhao L. (2013) Pharmacokinetics of single and multiple oral doses of arbidol in healthy Chinese volunteers. *Int. J. Clin. Pharmacol. Ther.* 51: 423–432. doi: 10.5414/CP201843
7. Hayden F. G., Sugaya N., Hirotsu N., Lee N., Jong M. D., Hurt A. C., Ishida T., Sekino H., Yamada K., Portsmouth S. (2018) Baloxavir Marboxil for Uncomplicated Influenza in Adults and Adolescents. *N Engl J Med.* 379: 913–923. DOI: 10.1056/NEJMoa1716197
8. Bright R. A., Medina M. J., Xu X., Perez-Oronoz G., Wallis T. R., Davis X. M., Povinelli L., Cox N. J., Klimov A. I. (2005) Incidence of adamantane resistance among influenza A (H3N2) viruses isolated worldwide from 1994 to 2005: A cause for concern. *The Lancet* 366: 1175–1181. DOI: 10.1016/S0140-6736(05)67338-2
9. Król E., Rychłowska M., Szewczyk B. (2014) Antivirals - current trends in fighting influenza. *Acta Biochim. Pol.* 61: 495–504. DOI: 10.18388/abp.2014\_1870
10. Sokolova A., Yarovaya O., Shernyukov A., Gatilov Y., Razumova Y., Zarubaev V., Tretiak T., Kiselev O., Salakhutdinov N. (2015) Discovery of a new class of antiviral compounds: Camphor imine derivatives. *Eur. J. Med. Chem.* 105: 263-273. DOI: 10.1016/j.ejmec.2015.10.010

11. Sokolova A., Yarovaya O., Baev D., Shernyukov A., Shtro A., Zarubaev V., Salakhutdinov N. (2017) Aliphatic and alicyclic camphor imines as effective inhibitors of influenza virus H1N1. *Eur. J. Med. Chem.* 127: 661-670. DOI: 10.1016/j.ejmech.2016.10.035
12. Sokolova A. S., Yarovaya O. I., Korchagina D. V., Zarubaev V. V., Tretiak T. S., Anfimov P. M., Kiselev O. I., Salakhutdinov N. F. (2014) Camphor-based symmetric diimines as inhibitors of influenza virus reproduction. *Bioorg. Med. Chem.* 22: 2141–2148, DOI: 10.1016/j.bmc.2014.02.038
13. Zarubaev V. V., Garshinina A. V., Tretiak T. S., Fedorova V. A., Shtro A. A., Sokolova A. S., Yarovaya O. I., Salakhutdinov N. F. (2015) Broad range of inhibiting action of novel camphor-based compound with anti-hemagglutinin activity against influenza viruses in vitro and in vivo. *Antivir. Res.* 120: 126–133. DOI: 10.1016/j.antiviral.2015.06.004
14. Sokolova A. S., Yarovaya O. I., Shernyukov A. V., Pokrovsky M.A., Pokrovsky A. G., Lavrinenko V. A., Zarubaev V. V., Tretiak T. S., Anfimov P. M., Kiselev O. I., Beklemishev A. B., Salakhutdinov N. F. (2013) New quaternary ammonium camphor derivatives and their antiviral activity , genotoxic effects and cytotoxicity. *Bioorg. Med. Chem.* 21: 6690–6698. DOI: 10.1016/j.bmc.2013.08.014
15. Sokolova A., Yarovaya O., Semenova M., Shtro A., Orshanskay Y., Zarubaev V., Salakhutdinov N. (2017) Synthesis and in vitro study of novel borneol derivatives as potent inhibitors of the influenza A virus. *Med. Chem. Commun.* 8: 960-963. DOI: 10.1039/C6MD00657D
16. Sokolova A., Yarovaya O., Shtro A., Borisova M., Morozova E., Tolstikova T., Zarubaev V., Salakhutdinov N. (2017) Synthesis and biological activity of heterocyclic borneol derivatives. *Chem. Heterocycl. Comp.* 53: 371-377. DOI: 10.1007/s10593-017-2063-3
17. Kononova A. A., Sokolova A. S., Cheresiz S. V., Yarovaya O. I., Nikitina R. A., Chepurnov A. A., Pokrovsky A. G., Salakhutdinov N. F. (2017) N-Heterocyclic borneol 17 derivatives as inhibitors of Marburg virus glycoprotein-mediated VSIV pseudotype entry. *Med. Chem. Commun.* 8: 2233-2237. DOI: 10.1039/C7MD00424A
18. Sokolova A. S., Yarovaya O. I., Zybkin A. V., Mordvinova E. D., Shcherbakova N. S., Zaykovskaya A. V., Baev D. S., Tolstikova T. G., Shcherbakov D. N., Pyankov O. V., Maksyutov R. A., Salakhutdinov N. F. (2020) Monoterpene-based inhibitors of filoviruses targeting the glycoprotein-mediated entry process. *Eur. J. Med. Chem.* 207:112726. doi.org/10.1016/j.ejmech.2020.112726
19. F. A Rey, Sh.-M. Lok. (2018) Common features of enveloped viruses and implications for immunogen design for next-generation vaccines. *Cell* 172: 1319-1334. doi.org/10.1016/j.cell.2018.02.054
20. Russell R. J., Kerry P. S., Stevens D. J., Steinhauer D. A., Martin S. R., Gamblin S. J., Skehel J. J. (2008) Structure of influenza hemagglutinin in complex with an inhibitor of membrane fusion. *Proc. Natl. Acad. Sci. USA* 105: 17736–17741. DOI: 10.1073/pnas.0807142105
21. Zarubaev V. V., Pushkina E. A., Borisevich S. S., Galochkina A. V., Garshinina A. V., Shtro A. A., Egorova A. A., Sokolova A. S., Khursan S. L., Yarovaya O. I., Salakhutdinov N. F. (2018) Selection of influenza virus resistant to the novel camphor-based antiviral camphecene results in loss of pathogenicity. *Virology* 524: 69–77. DOI: 10.1016/j.virol.2018.08.011

22. Maeda T., Ohnishi S. (1980) Activation of influenza virus by acidic media causes hemolysis and fusion of erythrocytes. *FEBS Lett.* 122: 283–287. doi.org/10.1016/0014-5793(80)80457-1
23. Berman H. M., Westbrook J., Feng Z., Gilliland G., Bhat T. N., Weissig H., Shindyalov I. N., Bourne P. E. (2000) The protein data bank. *Nucleic Acids Res.* 28: 235–242. DOI: 10.1093/nar/28.1.235
24. Harder E., Damm W. et al (2015) OPLS3: A Force Field Providing Broad Coverage of Drug-like Small Molecules and Proteins. *J. Chem. Theory Comput.* 12: 281–296. DOI: 10.1021/acs.jctc.5b00864
25. Gamblin S. J., Haire L. F. et al (2004) The Structure and Receptor Binding Properties of the 1918 Influenza Hemagglutinin. *Science* 303: 1838–1842. DOI: 10.1126/science.1093155

## Figures

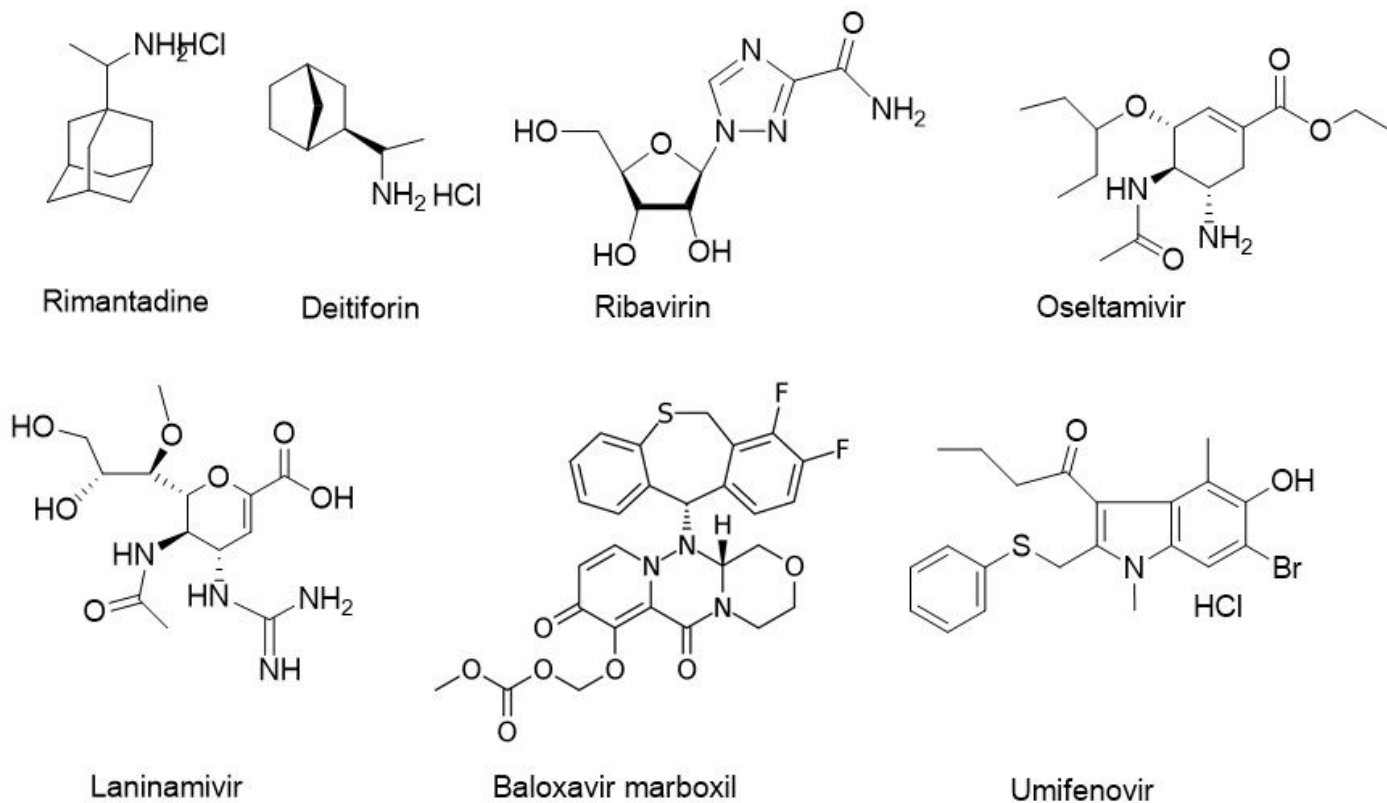


**Figure 1**

Anti-influenza drugs approved for clinical use to treat the influenza infection.

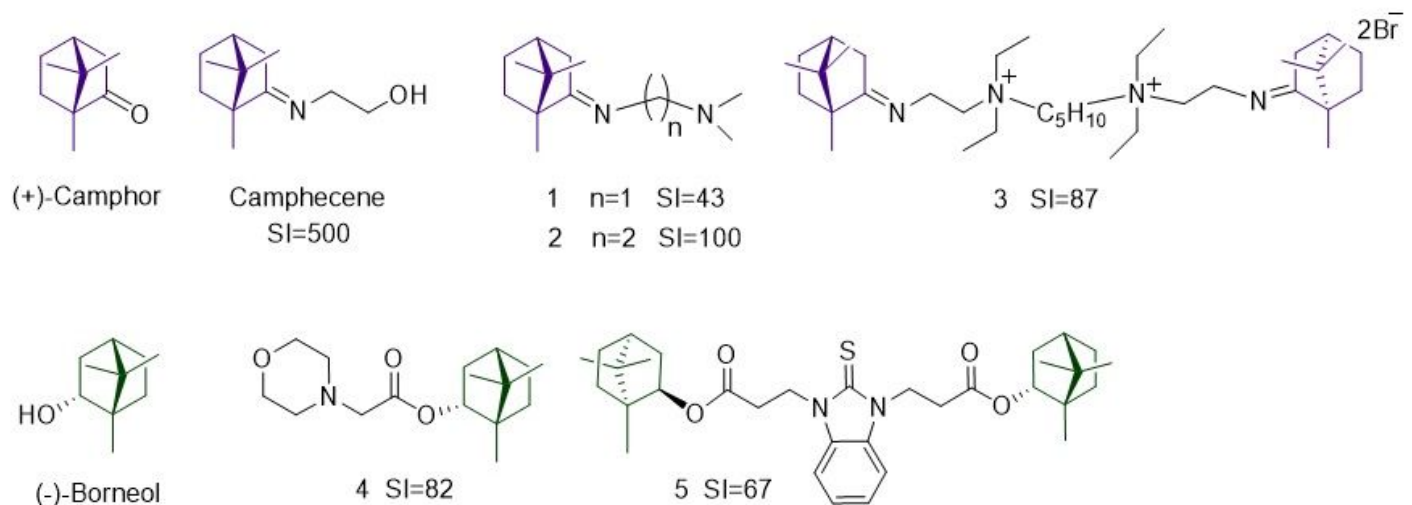


**Figure 2**

(+)-Camphor and (-)-borneol derivatives with potent activity against influenza viruses A(H1N1)pdm09. SI is the selectivity index.

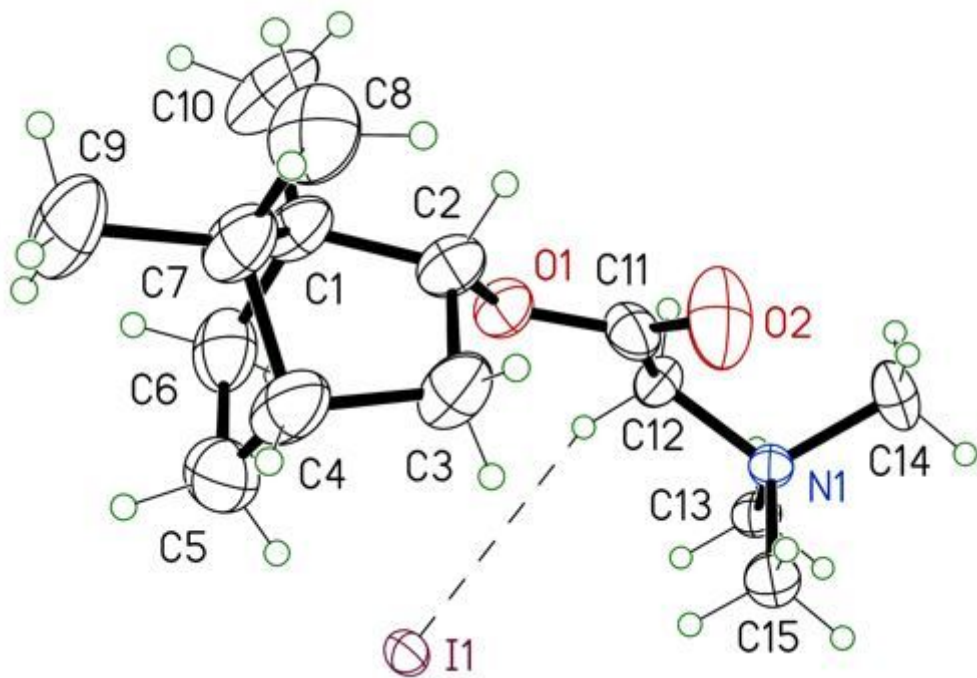


**Figure 3**

ORTEP representations of compound 10a, the displacement ellipsoids are drawn at a probability of 30%. Only one of the two independent molecules is shown.

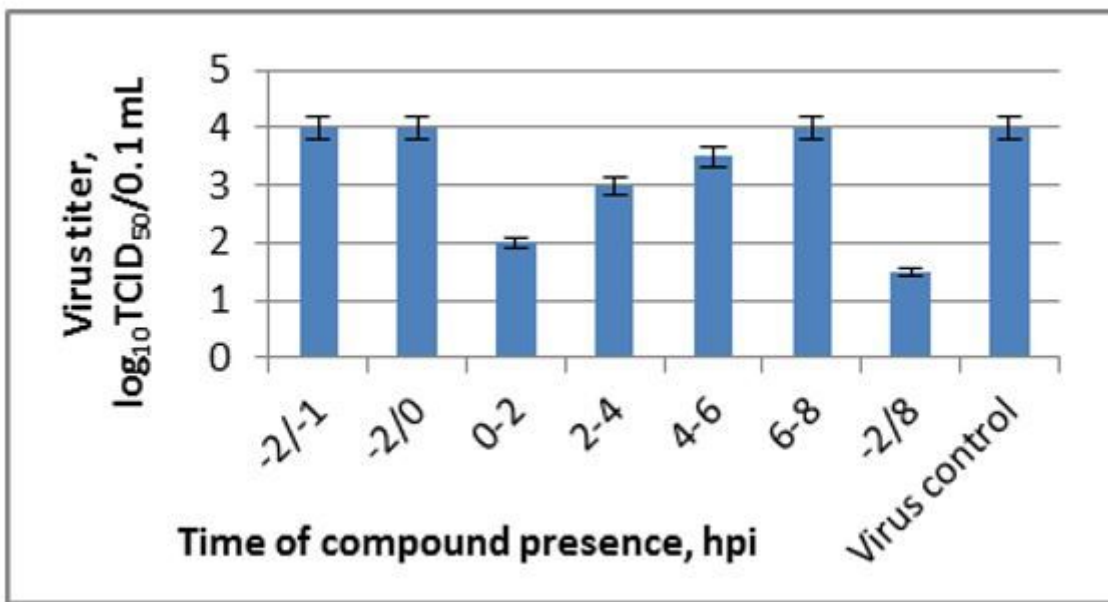


**Figure 4**

Time-of-addition activity of compound 10a against the influenza virus A/Puerto Rico/8/34 (H1N1). MDCK cells were infected with influenza virus, and salt 10a was added and removed at the indicated time points, where 0 corresponds to the moment when the cells were infected. The infectious activity of viral progeny was tested by further titration of the MDCK cells.

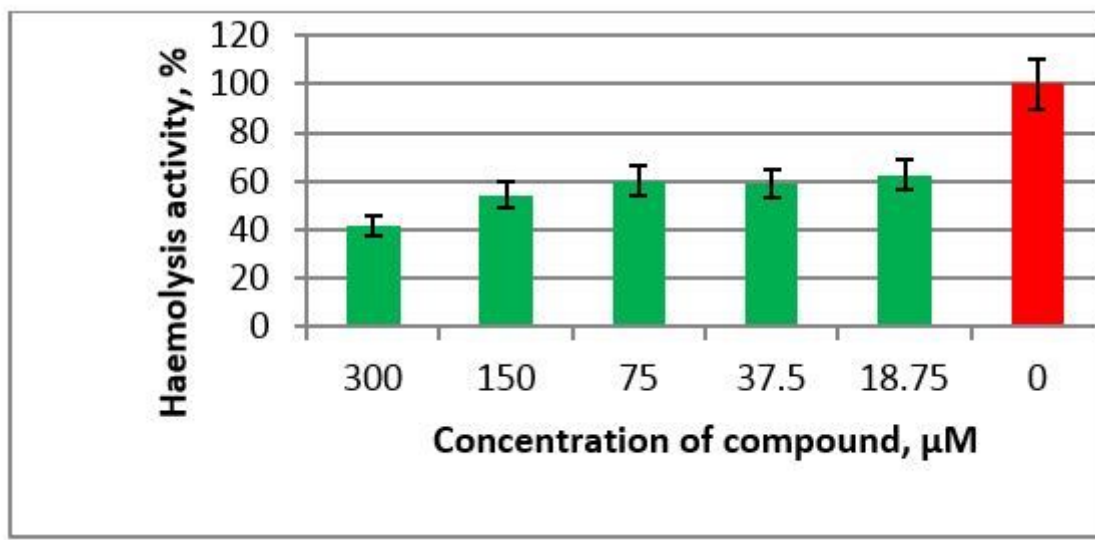


**Figure 5**

Haemagglutinin-inhibiting activity of compound 10a against influenza A virus HA. The compound was mixed with 128 hemagglutinating units of the influenza virus, incubated at room temperature for 30 min, mixed with 0.75% chicken erythrocytes and incubated at +4°C. After incubation with MES buffer (0.1 M MES, 0.15 M NaCl, 0.9 mM CaCl<sub>2</sub>, 0.5 mM MgCl<sub>2</sub>, pH 5.0) and sedimentation of erythrocytes, optical

density in the wells was measured at 405 nm. The HA-inhibiting activity of compound 10a was calculated comparing to HA activity of influenza A virus without additives.

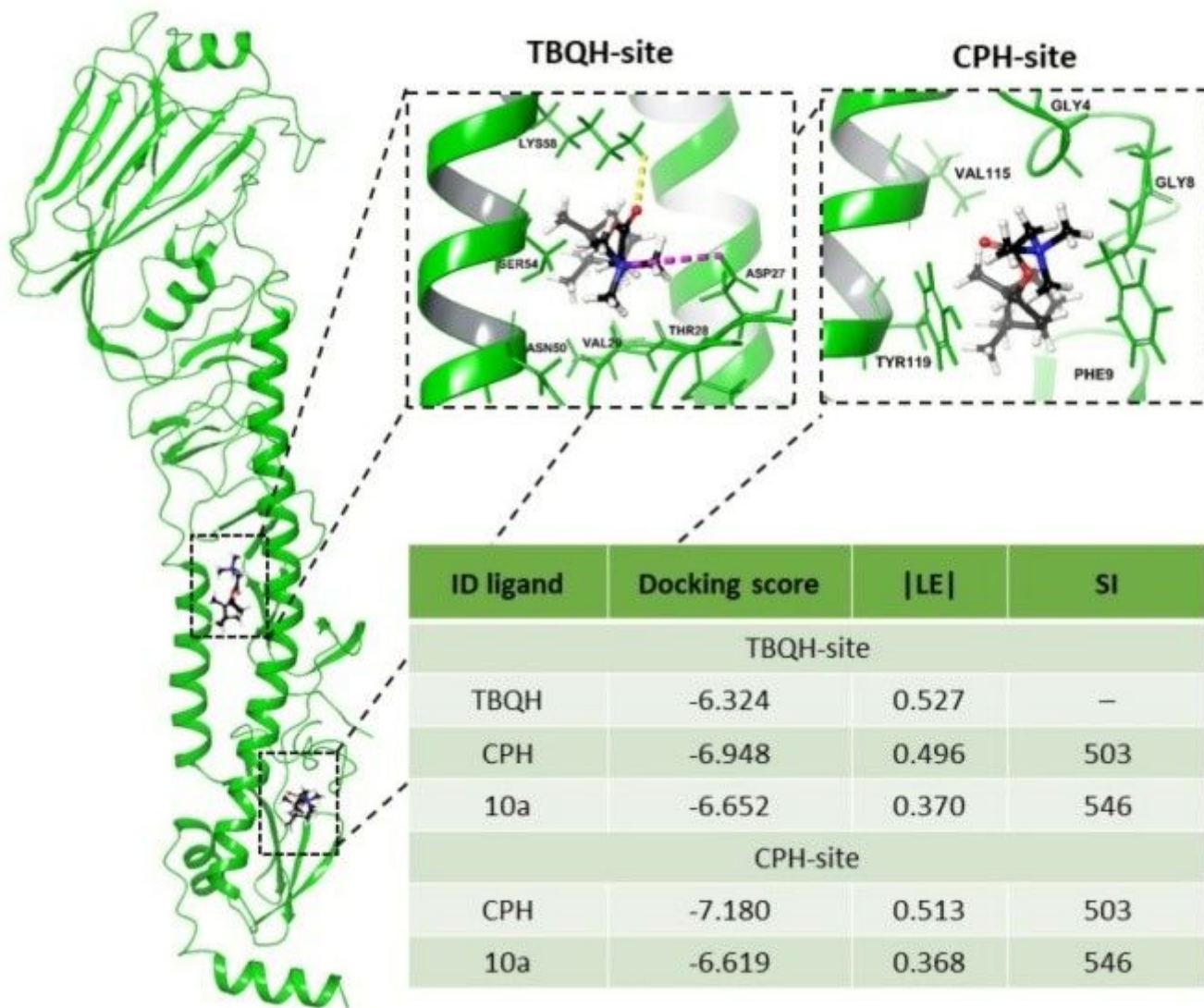


**Figure 6**

The location of the ligands in the binding sites of HA (PDB code 3LZG [28]). The H-bond and salt bridges are presented as yellow and pink dotted lines, respectively. The ligand efficiency (LE) is the ratio of the docking score to the number of heavy atoms (no hydrogen atoms).

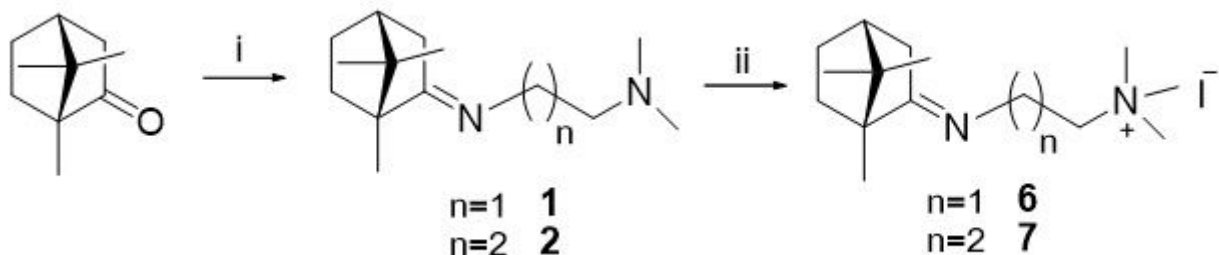


**Figure 7**

Reagents and conditions: (i) N,N-dimethylethylenediamine or N,N-dimethylpropane-1,3-diamine, ZnCl<sub>2</sub>, reflux under solvent-free conditions; (ii) CH<sub>3</sub>I, CH<sub>3</sub>CN, reflux.

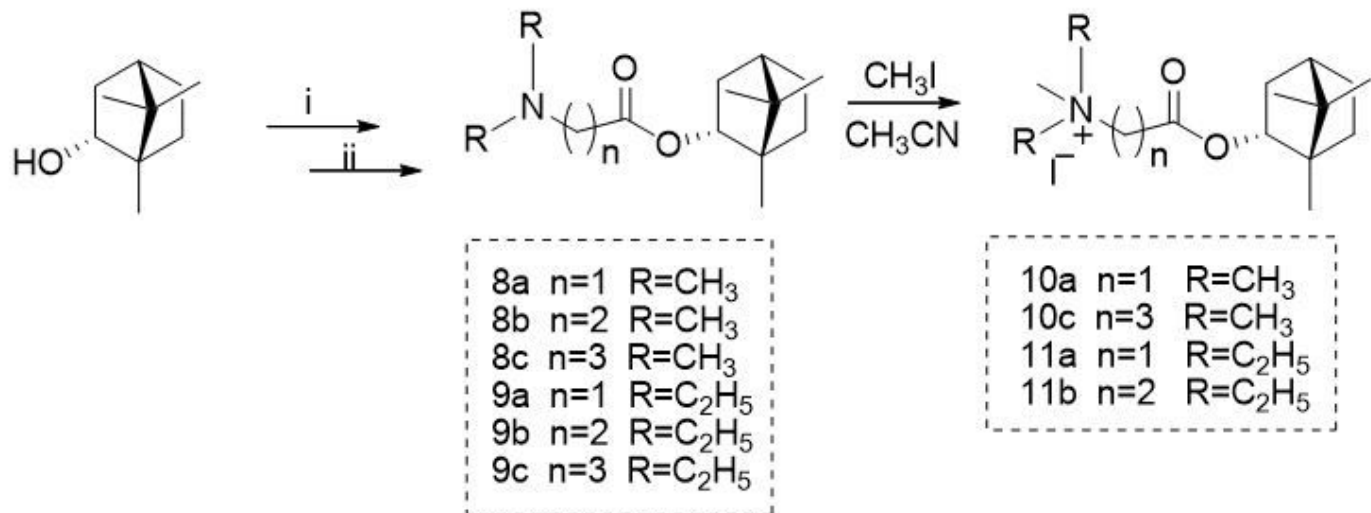


**Figure 8**

Synthesis of the (-)-borneol derivatives.

## Supplementary Files

This is a list of supplementary files associated with this preprint. Click to download.

- [Supplementary.docx](#)